Eur. Phys. J. D **31**, 91–100 (2004)
DOI: 10.1140/epjd/e2004-00121-4

THE EUROPEAN PHYSICAL JOURNAL D

Ion-acoustic solitons and double-layers in a plasma consisting of positive and negative ions with non-thermal electrons

T.S. Gill[1,a], P. Bala[1], H. Kaur[2], N.S. Saini[1], S. Bansal[1], and J. Kaur[1]

[1] Department of Physics, Guru Nanak Dev University, Amritsar-143005, India
[2] Department of Physics, Khalsa College, Amritsar-143002, India

Received 27 April 2004 / Received in final form 9 July 2004
Published online 21 September 2004 –

Abstract. In this research paper, the authors have studied the properties of ion-acoustic solitons and double-layers in a plasma consisting of warm positive and negative ions with different concentration of masses, charged states and non-thermal electrons using small amplitude approximation. Reductive perturbation method is used to derive KdV and m-KdV equations. Existence of ion-acoustic solitons and double-layer is explored over a wide range of parameter space. The role of non-thermal electrons characterized by finite β is investigated. It is observed that for a particular value of β, there is a transition from compressive to rarefactive solitons. However, when β is increased beyond a critical value, no double-layers are obtained. The significance of relative ion masses is also investigated.

PACS. 52.35.-g Waves, oscillations, and instabilities in plasmas and intense beams

1 Introduction

Nonlinear wave structures are beautiful and amazing manifestation of nature, arising out of competition between properties like nonlinearity, dispersion and dissipation. They have been paying rich dividends to researchers as they offer deep physical insight underlying the nonlinear phenomena. Space environment constitutes a magnificent laboratory for the investigation of plasma phenomena and nonlinear wave structures. To quote a few nonlinear wave structures, we have solitons, shock waves, double-layers etc. observed both in space and laboratory. In plasmas ion-acoustic solitons have been focus of most investigations. However, in the past two decades, the double-layers have also attracted a great deal of attention because of their relevance to cosmic applications [1–5]. Furthermore, space plasmas are of multispecies type and offer a rich source for studying the double-layers. Their relevance further stems from the fact that these are considered as the source of Earth's aurora. It was also discovered that the acoustic double-layers also are responsible for auroral electron precipitation. Moreover, electrostatic double-layers provide a mechanism for the acceleration of the particles.

To study nonlinear structures, we usually adopt some form of perturbation method. In small amplitude approximation, one ends up deriving some form of nonlinear partial differential equations like Korteweg-de-Vries (KdV) or modified Korteweg-de-Vries (m-KdV) or nonlinear Schroedinger equations etc. Using the reductive perturbation technique, ion-acoustic double-layers have been studied by a number of authors [6–9] in different plasma systems. In the past few years, there have been considerable interest in understanding the behaviour of multispecies plasma consisting of cold or warm positive and negative ions with usual Boltzmann's electrons. Ion-acoustic solitons and double-layers in multispecies plasma have been recently studied in a number of investigations [10–19]. However, it has been recently found that the electron and ion distributions play a crucial role in characterizing the physics of the wave structures. They offer considerable increase in richness and variety of wave motion which can exist in plasma and further significantly influence the conditions required for the formation of solitons and double-layers. Moreover, it is also known that electron and ion distributions can be significantly modified in the presence of large amplitude waves.

With observations of solitary wave structures with density depression, emphasizing the role of nonthermal electrons distribution on characterisation of solitary wave/solitons were reported [20,24–26]. Some other investigations have been reported in the study of ion-acoustic solitons in plasmas with non-Maxwellian electron distributions [21–23,27–29]. Nonthermal distributions are a common feature of the auroral zone [30]. Mechanism for the formation of non-thermal particles distributions in space plasma is still a central problem. The aim of the present investigation is to study how the non-thermal electron distributions influence the solitary wave behaviour as well as

[a] e-mail: nspst99@yahoo.com

the physics of ion-acoustic double-layers in a multispecies plasma consisting of positive ions, negative ions and non-thermal electrons. The organisation of the present paper is as follows: in Section 2, we set up basic equations governing the dynamics of the multispecies plasma. Section 3 is devoted to derive KdV equation. In Section 4, we obtain soliton solution while in Section 5, we derive m-KdV equation. In Section 6, we obtain double-layer solution under appropriate conditions and in Section 7, we present discussion of numerical computation of different plasma systems. In last section, we have summarized the various results obtained in the present investigation.

2 Basic equations

We consider a collisionless unmagnetised plasma consisting of non-thermal electron distribution, warm positive and negative ion species having temperatures T_1 and T_2 which are divided into two distinct groups. We assume that low frequency electrostatic waves propagate in the plasma.

To explain observation made from the Freja satellite, Cairns et al. [20] assumed a distribution of electrons which is non-thermal with an excess of energetic particles. The non-thermal distribution for electrons was later used by a number of authors in various investigations. The number density of the electron fluid, with non-thermal electrons is given by:

$$n_e = (1 - \beta\phi + \beta\phi^2)e^{\phi} \tag{1}$$

where

$$\beta = \frac{4\gamma}{1+3\gamma}.$$

Here γ is a parameter determining the number of non-thermal electrons present in our non-thermal plasma model [20,26,30]. This is non-Maxwellian distribution function which contains high energy electrons component. Such distributions are very common in auroral zone of ionosphere.

The nonlinear behaviour of the ion-acoustic waves may be described by the following set of normalized fluid equations:

$$\frac{\partial n_1}{\partial t} + \frac{\partial (n_1 v_1)}{\partial x} = 0 \tag{2}$$

$$\frac{\partial v_1}{\partial t} + v_1 \frac{\partial v_1}{\partial x} = -\frac{1}{\delta}\frac{\partial \phi}{\partial x} - \frac{\sigma_1}{\delta Z_1}\frac{1}{n_1}\frac{\partial n_1}{\partial x} \tag{3}$$

$$\frac{\partial n_2}{\partial t} + \frac{\partial (n_2 v_2)}{\partial x} = 0 \tag{4}$$

$$\frac{\partial v_2}{\partial t} + v_2 \frac{\partial v_2}{\partial x} = \frac{\epsilon_z}{\delta\eta}\frac{\partial \phi}{\partial x} - \frac{\sigma_2}{\delta\eta Z_1}\frac{1}{n_2}\frac{\partial n_2}{\partial x} \tag{5}$$

$$\frac{\partial^2 \phi}{\partial x^2} = n_e - \frac{n_1}{1-\alpha\epsilon_z} + \frac{\alpha\epsilon_z}{1-\alpha\epsilon_z} n_2 \tag{6}$$

where

$$\delta = \frac{\eta + \alpha\epsilon_z^2}{\eta(1-\alpha\epsilon_z)}, \quad \alpha = \frac{n_2^{(0)}}{n_1^{(0)}}, \quad \epsilon_z = \frac{Z_2}{Z_1},$$
$$\eta = \frac{m_2}{m_1}, \qquad \sigma_1 = \frac{T_1}{T_e}, \quad \sigma_2 = \frac{T_2}{T_e}. \tag{7}$$

In the above equations n_1, v_1 and n_2, v_2 are the densities and fluid velocities of positive and negative ion species respectively. $n_1^{(0)}$, $n_2^{(0)}$ are the equilibrium densities of two ion components respectively. Further, ϕ is the electrostatic potential. η is the mass ratio of the negative ion species to the positive ion species, α is the equilibrium density ratio of the negative ion to positive ion species and ϵ_z is the charge multiplicity ratio of the negative ion to positive ion species. In equations (1–6), velocities (v_1, v_2), potential (ϕ), time (t) and space coordinate (x) have been normalized with respect to the ion-acoustic speed in the mixture, C_s, thermal potential T_e/e, inverse of ion plasma frequency in the mixture ω_{pi}^{-1}, Debye length λ_D respectively. Ion densities n_1 and n_2 are normalized with their corresponding equilibrium values, whereas electron densities normalized by $n^{(0)}$. In the mixture, the ion-acoustic speed C_s, the ion plasma frequency ω_{pi} and the Debye length are respectively given by

$$C_s = \sqrt{\frac{T_e \delta Z_1}{m_1}}$$
$$\omega_{pi} = \sqrt{\frac{4\pi n^{(0)} e^2 Z_1 \delta}{m_1}} \tag{8}$$

and

$$\lambda_D = \sqrt{\frac{T_e}{4\pi n^{(0)} e^2}}. \tag{9}$$

3 Derivation of KdV equation

To study small but finite amplitude ion-acoustic solitary waves in our multispecies plasma model, we construct a weakly nonlinear theory of the ion-acoustic waves which lead to scaling of the independent variables through the stretched co-ordinates (ξ) and (τ):

$$\xi = \epsilon^{1/2}(x - \lambda_0 t) \tag{10}$$

$$\tau = \epsilon^{3/2} t \tag{11}$$

where ϵ is a small parameter measuring the weakness of the dispersion and λ_0 is the phase velocity of the wave to be determined later. Now to strike a balance between nonlinear and dispersive terms, we expand all dependent quantities in equations (1–6) around the equilibrium

values in powers of ϵ in the following form:

$$\begin{aligned} n_1 &= 1 + \epsilon n_1^{(1)} + \epsilon^2 n_1^{(2)} + \epsilon^3 n_1^{(3)} + ... \\ n_2 &= 1 + \epsilon n_2^{(1)} + \epsilon^2 n_2^{(2)} + \epsilon^3 n_2^{(3)} + ... \\ v_1 &= \epsilon v_1^{(1)} + \epsilon^2 v_1^{(2)} + \epsilon^3 v_1^{(3)} + ... \\ v_2 &= \epsilon v_2^{(1)} + \epsilon^2 v_2^{(2)} + \epsilon^3 v_2^{(3)} + ... \\ \phi &= \epsilon \phi^{(1)} + \epsilon^2 \phi^{(2)} + \epsilon^3 \phi^{(3)} + ... \end{aligned} \tag{12}$$

Substituting the expansion (12) into equations (1–6) and using equations (10, 11), equating terms with the same powers of ϵ we obtain a set of equations for ascending orders in ϵ as follows

$$(1-\beta)\phi^{(1)} - \frac{n_1^{(1)}}{(1-\alpha\epsilon_z)} + \frac{\alpha\epsilon_z}{1-\alpha\epsilon_z} n_2^{(1)} = 0 \tag{13}$$

$$\lambda_0 n_1^{(1)} = v_1^{(1)} \tag{14}$$

$$\lambda_0 n_2^{(1)} = v_2^{(1)} \tag{15}$$

$$\lambda_0 v_1^{(1)} = \frac{{\phi^{(1)}}^2}{\delta} + \frac{\sigma_1}{\delta Z_1} n_1^{(1)} \tag{16}$$

$$\lambda_0 v_2^{(1)} = \frac{\sigma_2}{\eta\delta Z_1} n_2^{(1)} - \frac{\epsilon_z}{\eta\delta}\phi^{(1)} \tag{17}$$

$$(1-\beta)\phi^{(2)} + \frac{{\phi^{(1)}}^2}{2} - \frac{n_1^{(2)}}{1-\alpha\epsilon_z} + \frac{\alpha\epsilon_z}{1-\alpha\epsilon_z} n_2^{(2)} = \frac{\partial^2\phi^{(1)}}{\partial\xi^2}. \tag{18}$$

Equations (14) to (17) are used to get the following first order quantities:

$$n_1^{(1)} = \frac{Z_1}{\delta Z_1\lambda_0^2 - \sigma_1}\phi^{(1)} \tag{19}$$

$$n_2^{(1)} = -\frac{Z_2}{\delta\eta Z_1\lambda_0^2 - \sigma_2}\phi^{(1)} \tag{20}$$

$$v_1^{(1)} = \frac{Z_1\lambda_0}{\delta Z_1\lambda_0^2 - \sigma_1}\phi^{(1)} \tag{21}$$

$$v_2^{(1)} = \frac{Z_2\lambda_0}{\delta\eta Z_1\lambda_0^2 - \sigma_2}\phi^{(1)}. \tag{22}$$

Similarly from the equations of continuity and equations of motion for positive and negative ions, we obtain the following equations to the next higher order of ϵ:

$$-\lambda_0\frac{\partial n_1^{(2)}}{\partial\xi} + \frac{\partial n_1^{(1)}}{\partial\tau} + \frac{\partial v_1^{(2)}}{\partial\xi} + \frac{\partial(n_1^{(1)}v_1^{(1)})}{\partial\xi} = 0 \tag{23}$$

$$-\lambda_0\frac{\partial n_2^{(2)}}{\partial\xi} + \frac{\partial n_2^{(1)}}{\partial\tau} + \frac{\partial v_2^{(2)}}{\partial\xi} + \frac{\partial(n_2^{(1)}v_2^{(1)})}{\partial\xi} = 0 \tag{24}$$

$$-\lambda_0\frac{\partial v_1^{(2)}}{\partial\xi} + \frac{\partial v_1^{(1)}}{\partial\tau} + v_1^{(1)}\frac{\partial v_1^{(1)}}{\partial\xi} = -\frac{1}{\delta}\frac{\partial\phi^{(2)}}{\partial\xi} - \frac{\sigma_1}{\delta Z_1}\frac{\partial n_1^{(2)}}{\partial\xi} + \frac{\sigma_1}{\delta Z_1} n_1^{(1)}\frac{\partial n_1^{(1)}}{\partial\xi} \tag{25}$$

$$-\lambda_0\frac{\partial v_2^{(2)}}{\partial\xi} + \frac{\partial v_2^{(1)}}{\partial\tau} + v_2^{(1)}\frac{\partial v_2^{(1)}}{\partial\xi} = \frac{\epsilon_z}{\eta\delta}\frac{\partial\phi^{(1)}}{\partial\xi} - \frac{\sigma_2}{\eta\delta Z_1}\frac{\partial n_2^{(2)}}{\partial\xi} + \frac{\sigma_2}{\eta\delta Z_1} n_2^{(1)}\frac{\partial n_2^{(1)}}{\partial\xi}. \tag{26}$$

On using equations (19) and (20) into equation (13), we get the following relation:

$$\frac{Z_1}{(1-\alpha\epsilon_z)}\left[\frac{1}{(\delta Z_1\lambda_0^2 - \sigma_1)} + \frac{\alpha\epsilon_z^2}{(\eta\delta Z_1\lambda_0^2 - \sigma_2)}\right] = 1-\beta. \tag{27}$$

It may be noted that equation (27) is quadratic in λ_0^2, therefore the inclusion of a finite ion temperature gives rise to two ion-acoustic modes propagating with different phase velocities. Apparently the modes are further significantly modified by the appearance of non-thermal electron distribution parameter β. The phase velocities of two modes is given by the following expression:

$$\lambda_{01}^2 = \left(\frac{1}{2(1-\beta)} + \frac{\sigma_2+\eta\sigma_1}{2\delta\eta Z_1}\right) - \sqrt{\left(\frac{1}{2(1-\beta)} + \frac{\sigma_2+\eta\sigma_1}{2\delta\eta Z_1}\right)^2 - \frac{1}{\eta\delta^2 Z_1}\left(\frac{\sigma_1\sigma_2}{Z_1} + \frac{\sigma_2+\sigma_1\alpha\epsilon_z^2}{1-\alpha\epsilon_z}\right)} \tag{28}$$

for slow ion-acoustic mode and

$$\lambda_{02}^2 = \left(\frac{1}{2(1-\beta)} + \frac{\sigma_2+\eta\sigma_1}{2\delta\eta Z_1}\right) + \sqrt{\left(\frac{1}{2(1-\beta)} + \frac{\sigma_2+\eta\sigma_1}{2\delta\eta Z_1}\right)^2 - \frac{1}{\eta\delta^2 Z_1}\left(\frac{\sigma_1\sigma_2}{Z_1} + \frac{\sigma_2+\sigma_1\alpha\epsilon_z^2}{1-\alpha\epsilon_z}\right)} \tag{29}$$

for fast ion-acoustic mode.

Apparently the phase velocities are the function of several parameters including density parameter (α), mass ratio parameters (η) and nonthermalcity (β) and ion temperatures σ_1, σ_2. Thus, the system supports two types of ion-acoustic modes which propagate with different phase velocities given by equations (28) and (29). The mode with smaller phase velocity is slow ion-acoustic mode whereas the mode with larger phase velocity is known as the fast ion-acoustic mode. Consequently, the system supports two types of ion-acoustic solitons, viz, slow ion-acoustic solitons and fast ion-acoustic solitons. Earlier investigations [19] reported two cases in which system does not support slow ion-acoustic mode viz.

(a) when both species are cold i.e., $\sigma_1 = \sigma_2 = 0$, substituting in equation (28) implies that $\lambda_{01}^2 = 0$, which clearly shows that slow ion-acoustic mode does not exist and fast acoustic mode exists i.e., equation (29) reduces to usual ion-acoustic mode;

(b) when $\sigma_1 = \sigma_2$, and $\eta = 1$, however, introduction of finite nonthermal electrons leads to the existence of slow ion-acoustic mode. Introduction of finite ion temperatures, when both ions have different temperatures, lead to the existence of both slow and fast ion-acoustic modes. As earlier reported, we have two soliton solutions. For the actual existence of slow ion-acoustic soliton, the phase velocity of slow ion-acoustic mode must be greater than the thermal velocity of the ions.

In such case, Landau damping will be small and we expect that slow ion-acoustic mode will not Landau damp. When phase velocity of a slow acoustic mode is comparable with thermal velocity of ions, then slow mode disappears. In the present investigation, for the chosen set of parameters and finite β, it is observed that phase velocity is greater than ion thermal velocities for both modes.

On differentiating equation (18), we get second order quantities which are eliminated in terms of first order quantities using equations (23–26). After a long algebraic but straightforward manipulations, we derive the following KdV equation:

$$\frac{\partial\phi^{(1)}}{\partial\tau} + C\phi^{(1)}\frac{\partial\phi^{(1)}}{\partial\xi} + D\frac{\partial^3\phi^{(1)}}{\partial\phi^3} = 0 \tag{30}$$

where $C = AB$ and $D = A/2$. Here A and B are given by

$$A = \frac{1-\alpha\epsilon_z}{\delta\lambda_0}\left[\frac{Z_1^2}{(\delta Z_1\lambda_0^2-\sigma_1)^2} + \frac{\alpha\eta Z_2^2}{(\eta\delta Z_1\lambda_0^2-\sigma_2)^2}\right]^{-1} \tag{31}$$

$$B = \frac{Z_1^2}{2(1-\alpha\epsilon_z)}\left[\frac{(3\delta Z_1\lambda_0^2-\sigma_1)}{(\delta Z_1\lambda_0^2-\sigma_1)^3} - \alpha\epsilon_z^3\frac{(3\eta\delta Z_1\lambda_0^2-\sigma_2)}{(\eta\delta Z_1\lambda_0^2-\sigma_2)^3}\right] - \frac{1}{2}. \tag{32}$$

Coefficient C being a function of a number of parameters, is a measure of nonlinearity, while coefficient D is the measure of dispersion. Further, non-thermal parameter appears in C and D through equations (28) and (29) and both these coefficients vary over a wide range of parameter space. It is possible to strike a delicate balance between nonlinearity and dispersive property, leading to formation of KdV soliton.

4 Soliton solution

The steady state solution of KdV equation (30) is obtained by transforming the independent variables ξ and τ as

$$\chi = \xi - u\tau \tag{33}$$

where u is a normalized constant velocity. Using equation (33) into (30) and integrating w.r.t. χ, we get

$$\frac{1}{2}\left(\frac{d\phi}{d\chi}\right)^2 + V(\phi) = 0 \tag{34}$$

where $\phi^{(1)}$ is replaced by ϕ for the sake of convenience and $V(\phi)$ is the Sagdeev potential given by

$$V(\phi) = \frac{1}{D}\left(\frac{C}{6}\phi^3 - \frac{u}{2}\phi^2\right). \tag{35}$$

It may be noted that in deriving equation (35), we have used the following boundary conditions:

$$\chi \to \pm\infty, \quad \left(\phi, \frac{d\phi}{d\chi}, \frac{d^2\phi}{d\chi^2}\right) \to 0. \tag{36}$$

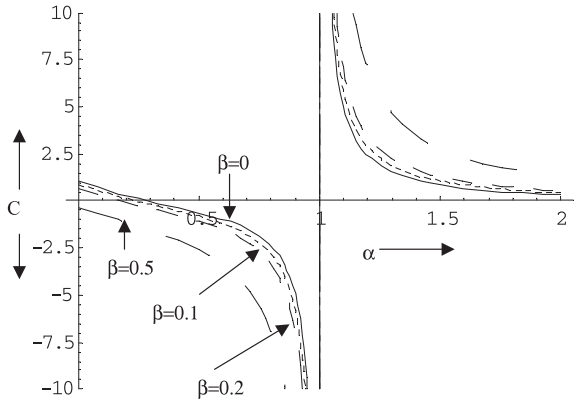

Fig. 1. Plot of nonlinearity coefficient C vs. α for different values of β with $\eta = 1$, $\sigma_1 = 0.1$, $\sigma_2 = 0.01$, and $Z_1 = Z_2 = 1$.

However, for the soliton solution, the Sagdeev potential V(ϕ) should be negative between $\phi = 0$ and $\phi = \phi_m$, where ϕ_m is some maximum or minimum value for the compressive and rarefactive solitons respectively. The boundary conditions on the Sagdeev potential should be satisfied as:

$$\begin{aligned} &V(\phi) = 0 \quad \text{at} \quad \phi = 0 \quad \text{and} \quad \phi = \phi_m \\ &V'(\phi) = 0 \quad \text{at} \quad \phi = 0 \\ &V'(\phi) > 0 \quad \text{at} \quad \phi = \phi_m \quad \text{for compressive soliton,} \\ \text{and} \quad &V'(\phi) < 0 \quad \text{at} \quad \phi = \phi_m \quad \text{for rarefactive soliton.} \end{aligned} \tag{37}$$

The soliton solution for equation (34) is given by

$$\phi = \phi_m \text{sech}^2 d^{-1}(\xi - u\tau) \tag{38}$$

where the amplitude ϕ_m and width d are given by

$$\phi_m = \frac{3u}{C} \tag{39}$$

and

$$d = \sqrt{\frac{2A}{u}}. \tag{40}$$

5 Derivation of m-KdV equation

There is singularity, when coefficient of nonlinear term of KdV equation is zero as shown in Figure 1. In this case, KdV soliton is not valid solution and we derive m-KdV equation. For this purpose, we include higher order effects, which are important in the study of double-layers. We introduce the following stretching coordinates (ξ) and (τ);

$$\xi = \epsilon(x - \lambda_0 t) \tag{41}$$

$$\tau = \epsilon^3 t. \tag{42}$$

On substituting the expansion (41) and (42) into equations (2–6), using equation (12), we obtain earlier results.

We therefore seek next order terms i.e. $O(\epsilon^3)$ of equations (2–5) and using the first order solutions, we get the following second order solutions

$$n_1^{(2)} = \frac{Z_1}{(\delta Z_1\lambda_0^2-\sigma_1)}\left[\frac{Z_1}{2}\frac{(3\delta Z_1\lambda_0^2-\sigma_1)}{(\delta Z_1\lambda_0^2-\sigma_1)^2}\phi^{(1)^2}+\phi^{(2)}\right] \tag{43}$$

$$n_2^{(2)} = \frac{Z_2}{(\delta\eta Z_1\lambda_0^2-\sigma_2)}\left[\frac{Z_2}{2}\frac{(3\delta\eta Z_1\lambda_0^2-\sigma_2)}{(\delta\eta Z_1\lambda_0^2-\sigma_2)^2}\phi^{(1)^2}-\phi^{(2)}\right] \tag{44}$$

$$v_1^{(2)} = \frac{Z_1}{2\delta\lambda_0}\frac{1}{(\delta Z_1\lambda_0^2-\sigma_1)}\left[1+\sigma_1\frac{(3\delta Z_1\lambda_0^2-\sigma_1)}{(\delta Z_1\lambda_0^2-\sigma_1)^2}\right]\phi^{(1)^2} + \frac{1}{\delta\lambda_0}\left[1+\frac{\sigma_1}{(\delta Z_1\lambda_0^2-\sigma_1)}\right]\phi^{(2)} \tag{45}$$

$$v_2^{(2)} = \frac{\epsilon_z}{2\delta\eta\lambda_0}\frac{Z_2}{(\delta\eta Z_1\lambda_0^2-\sigma_2)}\left[1+\sigma_2\frac{(3\delta\eta Z_1\lambda_0^2-\sigma_2)}{(\delta\eta Z_1\lambda_0^2-\sigma_2)^2}\right]\phi^{(1)^2} - \frac{\epsilon_z}{\delta\eta\lambda_0}\left[1+\frac{\sigma_2}{(\delta\eta Z_1\lambda_0^2-\sigma_2)}\right]\phi^{(2)}. \tag{46}$$

Poisson equation at $O(\epsilon^2)$ gives

$$Q\phi^{(1)^2} = 0 \tag{47}$$

where

$$Q = \frac{Z_1^2}{2(1-\alpha\epsilon_z)}\left[\frac{(3\delta Z_1\lambda_0^2-\sigma_1)}{(\delta Z_1\lambda_0^2-\sigma_1)^3} -\alpha\epsilon_z^3\frac{(3\eta\delta Z_1\lambda_0^2-\sigma_2)}{(\eta\delta Z_1\lambda_0^2-\sigma_2)^3}\right]-\frac{1}{2}. \tag{48}$$

Since $\phi^{(1)}\neq 0$, therefore "Q" should be at least of the order of ϵ and now "$Q\phi^{(1)^2}$" becomes of the order of ϵ^3; so it should be included in the next order of Poisson's equation. The next higher order, i.e. $O(\epsilon^3)$ of the Poisson equation on using first and second order solutions gives the following m-KdV equation

$$P\frac{\partial\phi^{(1)}}{\partial\tau}+Q\frac{\partial\phi^{(1)^2}}{\partial\xi}+R\frac{\partial\phi^{(1)^3}}{\partial\xi}+\frac{\partial^3\phi^{(1)}}{\partial\xi^3}=0 \tag{49}$$

where

$$P = \frac{2\delta Z_1^2\lambda_0}{(1-\alpha\epsilon_z)}\left[\frac{1}{(\delta Z_1\lambda_0^2-\sigma_1)^2}+\alpha\epsilon_z^2\frac{\eta}{(\eta Z_1\lambda_0^2-\sigma_2)^2}\right] \tag{50}$$

and

$$R = \frac{1}{(1-\alpha\epsilon_z)}\frac{Z_1^3}{(\delta Z_1\lambda_0^2-\sigma_1)^3} \times\left[1+\frac{(3\delta Z_1\lambda_0^2-\sigma_1)(\delta Z_1\lambda_0^2+\sigma_1)}{2(\delta Z_1\lambda_0^2-\sigma_1)^2}+\frac{\sigma_1}{3(\delta Z_1\lambda_0^2-\sigma_1)}\right] + \frac{1}{(1-\alpha\epsilon_z)}\frac{\alpha\epsilon_z Z_2^3}{(\eta\delta Z_1\lambda_0^2-\sigma_2)^3} \times\left[1+\frac{(3\eta\delta Z_1\lambda_0^2-\sigma_2)(\eta\delta Z_1\lambda_0^2+\sigma_2)}{2(\eta\delta Z_1\lambda_0^2-\sigma_2)^2}+\frac{\sigma_2}{3(\eta\delta Z_1\lambda_0^2-\sigma_2)}\right] - \frac{1+3\beta}{6}. \tag{51}$$

6 Double-layer solution

In this section, we present double-layer solution associated with the mixed m-KdV equation (49). For this purpose, we introduce a variable $\zeta=\xi-u\tau$ in a stationary frame, where u is a constant velocity. Equation (49) now becomes:

$$\frac{1}{2}\left(\frac{d\phi}{d\zeta}\right)^2+V(\phi)=0 \tag{52}$$

where $V(\phi)$ is the Sagdeev potential given by

$$V(\phi)=-\frac{1}{2}Pu\phi^2+\frac{1}{3}Q\phi^3+\frac{1}{4}R\phi^4. \tag{53}$$

Here while deriving equation (52), we have used the boundary conditions that

$$\phi\to 0,\ \ \frac{d\phi}{d\zeta},\ \ \frac{d^2\phi}{d\zeta^2}\to 0 \quad \text{as} \quad |\zeta|\to\infty.$$

Further, equation (52) with equation (53) can be considered as an equation of motion of a particle of unit mass under the action of the potential function $V(\phi)$. It may also be imagined as an equation of anharmonic oscillator provided that we interpret ζ and ϕ as time and space coordinates respectively. For double-layer solution, the Sagdeev potential should be negative between $\phi=0$ and ϕ_m, where ϕ_m is some extremum value of potential. Additional boundary conditions that $V(\phi)$ should satisfy for double-layer solution are follows:

$$\begin{aligned} V(\phi)&=0 \quad \text{at} \quad \phi=0 \quad \text{and} \quad \phi=\phi_m,\\ V'(\phi)&=0 \quad \text{at} \quad \phi=0 \quad \text{and} \quad \phi=\phi_m,\\ V''(\phi)&<0 \quad \text{at} \quad \phi=0 \quad \text{and} \quad \phi=\phi_m. \end{aligned} \tag{54}$$

Applying the first two boundary conditions of equation (54) in equation (53) we obtain

$$u=\left(\frac{-R}{2P}\right)\phi_m^2 \tag{55}$$

and

$$\phi_m=-\frac{2Q}{3R}. \tag{56}$$

Using equations (55) and (56) in equation (53), we get

$$V(\phi)=\frac{R\phi^2}{4}(\phi_m-\phi)^2. \tag{57}$$

The double-layer solution of equation (49) is given by

$$\phi=\frac{\phi_m}{2}\left[1-\tanh\sqrt{\frac{-R}{8}}\phi_m(\xi-u\tau)\right]. \tag{58}$$

It may be noted from the above equation that for the existence of a double-layer, the coefficient of cubic non linear term of the m-KdV equation i.e., R should be negative. It may also be noted from equation (56) that the nature of the double-layer i.e., whether the system will support

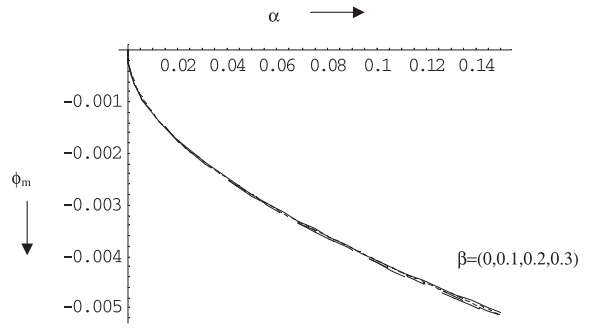

Fig. 2. Variation of slow ion-acoustic soliton amplitude ϕ_m with α for different values of β with the following set of parameters: $\eta = 1$, $\sigma_1 = 0.1$, $\sigma_2 = 0.0$, $Z_1 = Z_2 = 1$, and $u = 0.01$.

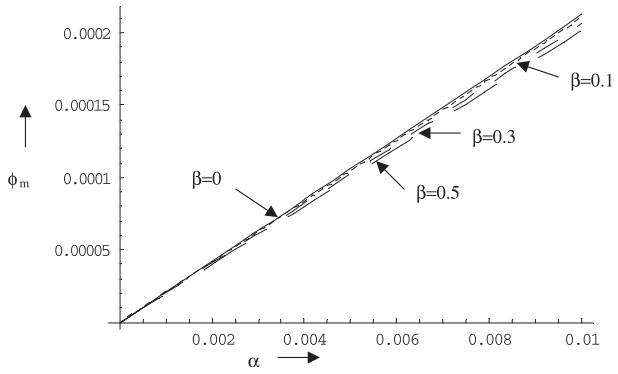

Fig. 3. Variation of slow ion-acoustic soliton amplitude ϕ_m with α for different values of β with the following set of parameters: $\eta = 1$, $\sigma_1 = 0.0$, $\sigma_2 = 0.1$, $Z_1 = Z_2 = 1$, and $u = 0.01$.

a compressive or rarefactive double-layer, depends on the sign of Q. If Q is positive, a compressive double-layer exists whereas for negative Q, a rarefactive double-layer exists. The thickness d of the double-layer is given by

$$d = \frac{4\sqrt{\frac{-2}{R}}}{|\phi_m|}. \tag{59}$$

7 Discussion

The (H^+, O_2^-) and (H^+, H^-) plasmas occur in the D-region of the ionosphere. For these type of plasmas, we have numerically evaluated ϕ_m as a function of α for different values of β and results for slow ion-acoustics modes are shown in Figures 2 and 3. For slow ion-acoustic mode, relative temperature of the two species and finite β are relevant parameters. It is observed that when the temperature of positive ion is finite but the negative is cold, there is only one mode of rarefactive type and is independent of β. However, when the temperature of the negative ion is finite but positive ions are cold, then for particular density ratio α, the maximum amplitude of compressive slow ion-acoustic soliton decreases with increase in β. For the fast acoustic mode relative density as well as finite β are relevant parameters, we have computed ϕ_m as function

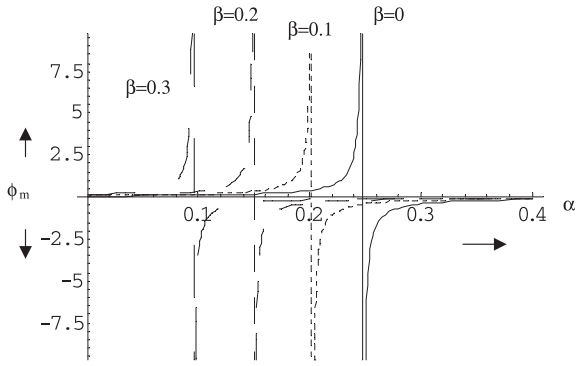

Fig. 4. Variation of fast ion-acoustic soliton amplitude ϕ_m with α for different values of β with the following set of parameters: $\eta = 1$, $\sigma_1 = 0.01$, $\sigma_2 = 0.05$, $Z_1 = Z_2 = 1$, and $u = 0.01$.

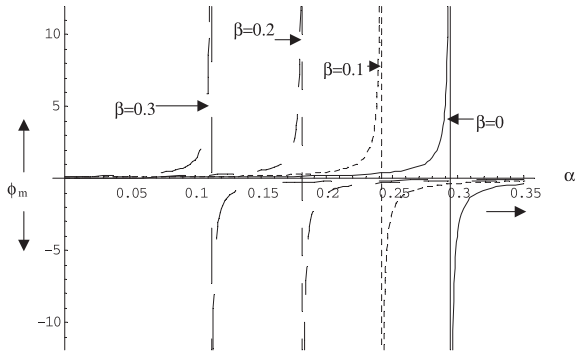

Fig. 5. Variation of fast ion-acoustic soliton amplitude ϕ_m with α for different values of β with the following set of parameters: $\eta = 1$, $\sigma_1 = 0.01$, $\sigma_2 = 0.0$, $Z_1 = Z_2 = 1$, and $u = 0.01$.

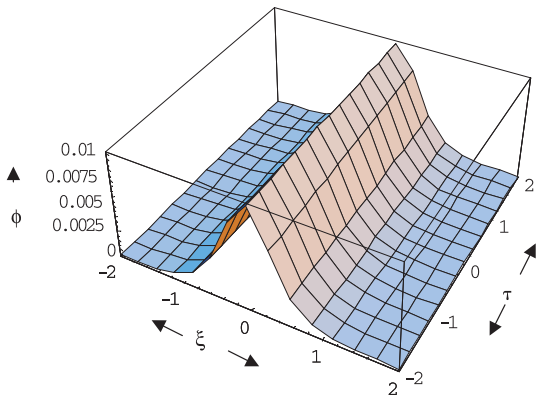

Fig. 6. 3D plot of slow ion-acoustic soliton for ϕ vs. ξ and τ with the following set of parameters: $\alpha = 0.2$, $\beta = 0.1$, $\eta = 1$, $\sigma_1 = 0.1$, $\sigma_2 = 0.01$, $Z_1 = Z_2 = 1$, and $u = 0.02$.

of α for fast ion-acoustic mode for different values of β and plotted graphs as shown in Figures 4 and 5. We find that both compressive as well as rarefactive solitons exist. With the increase in nonthermalcity, there is transition with β and maximum amplitude occurs for low relative density concentration. This feature is succinctly displayed in Figures 4 and 5.

In Figures 6 and 7, we show a three dimensional profile of solitons, where ϕ as function of ξ and η is plotted for

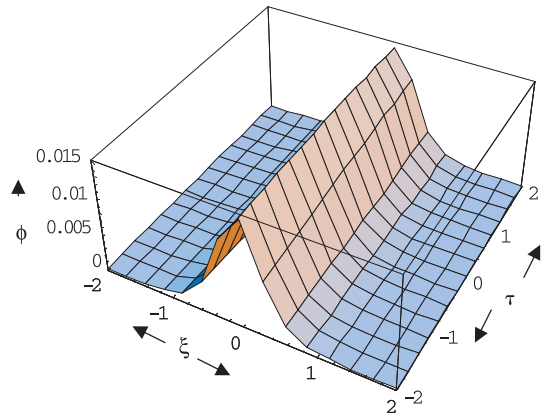

Fig. 7. 3D plot of slow ion-acoustic soliton for ϕ vs. ξ and τ with the following set of parameters: $\alpha = 0.2$, $\beta = 0.1$, $\eta = 1$, $\sigma_1 = 0.1$, $\sigma_2 = 0.01$, $Z_1 = Z_2 = 1$, and $u = 0.03$.

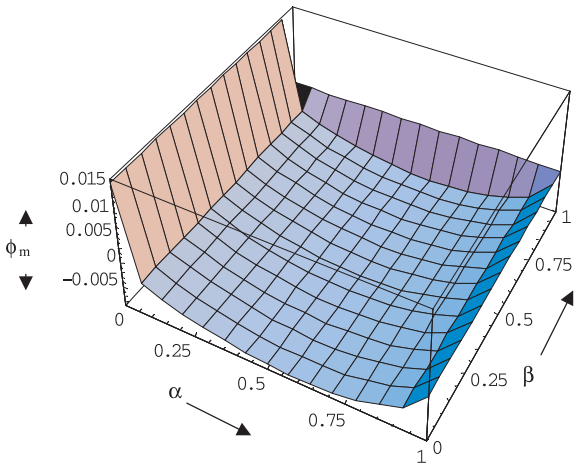

Fig. 8. 3D plot of slow ion-acoustic soliton for ϕ_m vs. α and β with the following set of parameters: $\eta = 1$, $\sigma_1 = 0.1$, $\sigma_2 = 0.01$, $Z_1 = Z_2 = 1$, and $u = 0.01$.

two values of u. It is observed that with the increase of u the maximum amplitude increases.

3D profile of KdV slow and fast modes are shown in Figures 8 and 9, where ϕ_m as a function of α and β are displayed. Similarly 3D portrait of double-layer solution is shown in Figure 10.

For (H^+, H^-), we have performed numerical computation of $V(\phi)$ vs. ϕ for various ranges of parameters. The results are shown in the form of graphs. In Figures 11 and 12, where we have taken density ratio parameter $\alpha = 0.2$ and $\alpha = 0.4$, while the temperatures $\sigma_1 = 0.1$ and $\sigma_2 = 0.01$ are same for both of these figures. Other parameters are as follows: $\eta = 1$ and $u = 0.01$.

Here, we observe the effect of non-thermal electrons in characterization of solitons. In the absence of non-thermal electrons ($\beta = 0$), only compressive solitons are obtained. However, when β is increased to $\beta = 0.1$, amplitude of compressive solitons and depth of potential are increased. But with further increase of β, we obtain a transition in which only rarefactive solitons are observed which disappeared on further increasing β. To observe this transition,

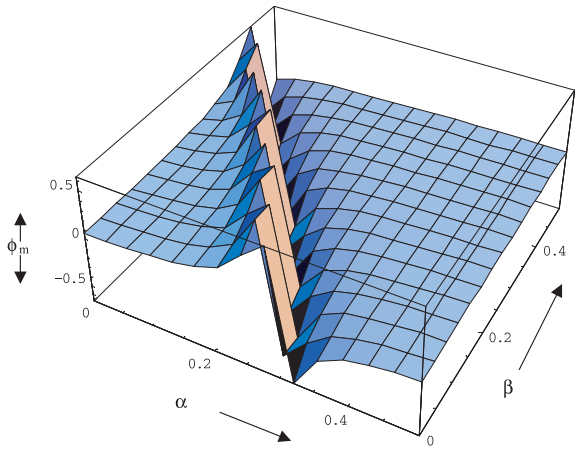

Fig. 9. 3D plot of fast ion-acoustic soliton for ϕ_m vs. α and β with the following set of parameters: $\eta = 1$, $\sigma_1 = 0.1$, $\sigma_2 = 0.01$, $Z_1 = Z_2 = 1$, and $u = 0.01$.

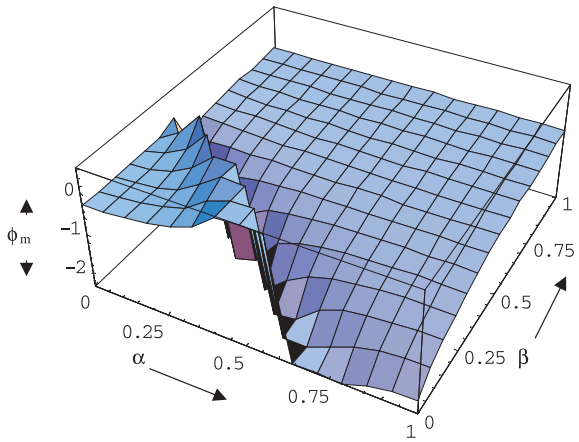

Fig. 10. 3D plot of fast ion-acoustic double-layer for ϕ_m vs. α and β with $\eta = 1$, $\sigma_1 = 0.1$, $\sigma_2 = 0.01$ and $Z_1 = Z_2 = 1$.

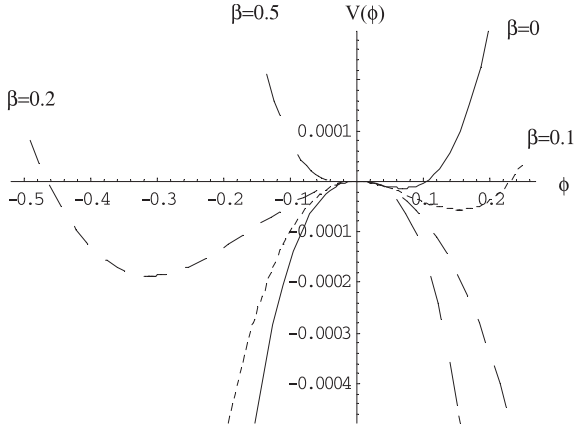

Fig. 11. Variation of Sagdeev potential of solitons $V(\phi)$ with ϕ for different values of β with the following set of parameters: $\alpha = 0.2$, $\eta = 1$, $\sigma_1 = 0.1$, $\sigma_2 = 0.01$, $Z_1 = Z_2 = 1$, $u = 0.01$.

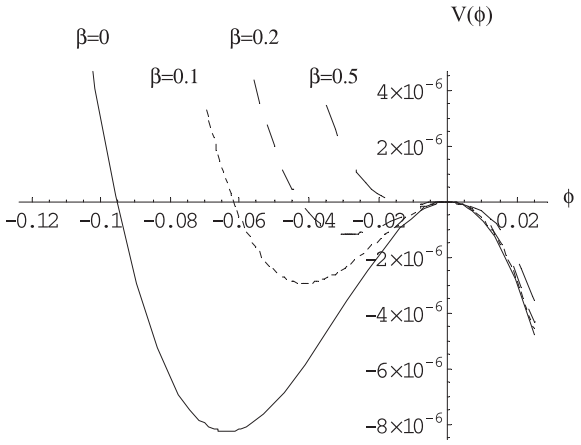

Fig. 12. Variation of Sagdeev potential of solitons $V(\phi)$ with ϕ for different values of β with the following set of parameters: $\alpha = 0.4$, $\eta = 1$, $\sigma_1 = 0.1$, $\sigma_2 = 0.01$, $Z_1 = Z_2 = 1$, $u = 0.01$.

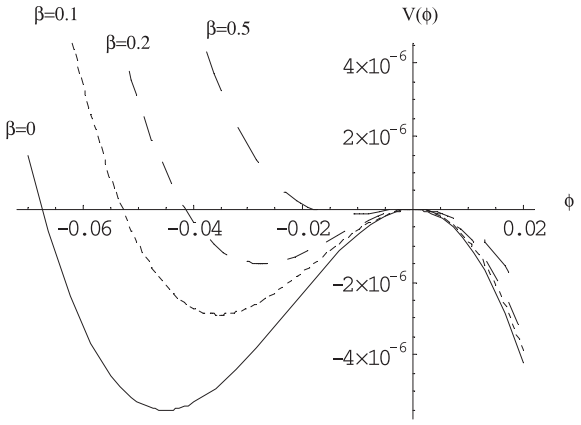

Fig. 13. Variation of Sagdeev potential of solitons $V(\phi)$ with ϕ for different values of β with the following set of parameters: $\alpha = 0.2$, $\eta = 0.476$, $\sigma_1 = 0.1$, $\sigma_2 = 0.01$, $Z_1 = Z_2 = 1$, $u = 0.01$.

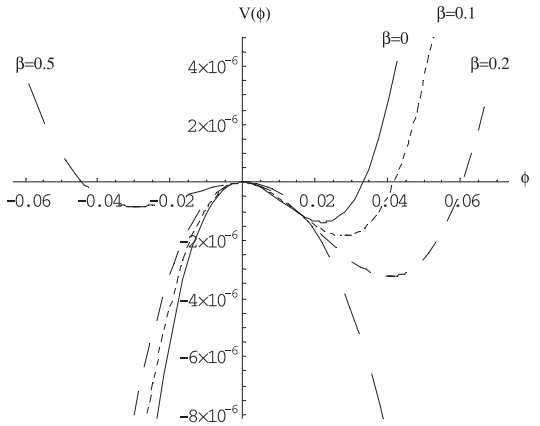

Fig. 14. Variation of Sagdeev potential of solitons $V(\phi)$ with ϕ for different values of β with the following set of parameters: $\alpha = 0.2$, $\eta = 32$, $\sigma_1 = 0.1$, $\sigma_2 = 0.01$, $Z_1 = Z_2 = 1$, $u = 0.01$.

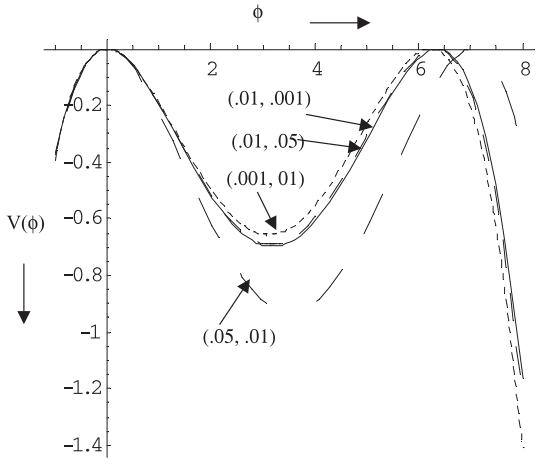

Fig. 15. Variation of Sagdeev potential ion-acoustic double-layers $V(\phi)$ with ϕ for different values of (σ_1, σ_2) with the following set of parameters: $\alpha = 0.65$, $\eta = 1.9$, $\beta = 0$, $Z_1 = Z_2 = 1$.

we have numerically calculated coefficient of nonlinear term as a function of α for different values of nonthermal parameter β and the results are shown in the form of graphs in Figure 1. The curve for $\beta = 0.5$ clearly represents the transition for chosen set of parameters. In case of $\alpha = 0.4$, we observe only rarefactive solitons as depicted in Figure 12. In this case, the maximum amplitude and depth of well decrease with the increase of β. Thus, the increase of density ratio or density of negative ions, leads to the formation of rarefactive solitons.

The (Ar^+, F^-) plasma has been used in experimental studies of ion-acoustic wave propagation in a number of investigations [31–33]. This plasma composition has been used in the experimental investigation of strong double-layers [34]. Here we have also done numerical computation of $V(\phi)$ vs. ϕ for (Ar^+F^-) plasma and taken the following realistic parameters: $\alpha = 0.2$, $\sigma_1 = 0.1$, $\sigma_2 = 0.01$, $u = 0.01$ and $\beta = 0$, 0.1, 0.2, 0.5. Results are exhibited in the form of graphs as shown in Figure 13. Only rarefactive solitons are obtained for all the values of non-thermal parameters from $\beta = 0$ to $\beta = 0.5$. Further, the peak amplitude and the depth of potential decrease with increase in the value of β. This behaviour compares well with that obtained for (H^+, H^-) plasma in Figure 12. Maximum peak amplitude is obtained in the absence of non-thermal electrons. Thus, the presence of non-thermal electrons restricts the range of parameter space for obtaining solitons. Further, the mass ratio and nonthermalcity play crucial role in characterising the soliton. From Figures 11 and 13, it is clear that with decrease of mass ratio, only rarefactive solitons are observed. Further increase of the density ratio results in compressive soliton.

Soliton behaviour is observed in (H^+, O_2^-) plasmas and shown in Figure 14, in which we have plotted $V(\phi)$ vs. ϕ for various values of β and for $\sigma_1 = 0.1$, $\sigma_2 = 0.01$, while $\alpha = 0.2$. For low values of β, compressive solitons are observed whereas higher $\beta = 0.5$ leads to appearance of rarefactive solitons. On the other hand, increase of mass ratio leads to appearance of compressive solitons and non-thermal parameters clearly play an important role. This is highlighted in Figure 14.

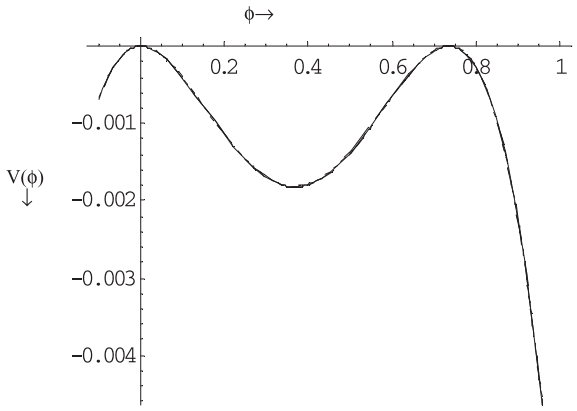

Fig. 16. Variation of Sagdeev potential ion-acoustic double-layers $V(\phi)$ with ϕ for different values of (σ_1, σ_2) with the following set of parameters: $\alpha = 0.65$, $\eta = 1.9$, $\beta = 0.5$, $Z_1 = Z_2 = 1$.

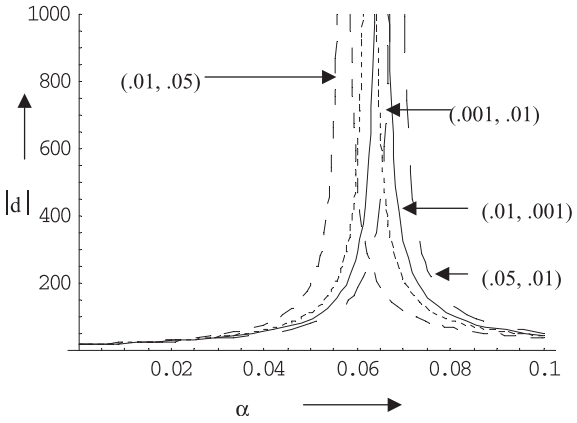

Fig. 17. Variation of width $|d|$ of ion-acoustic double-layers with density ratio α for different values of (σ_1, σ_2) with the following set of parameters: $\eta = 0.476$, $\beta = 0.2$, $Z_1 = Z_2 = 1$.

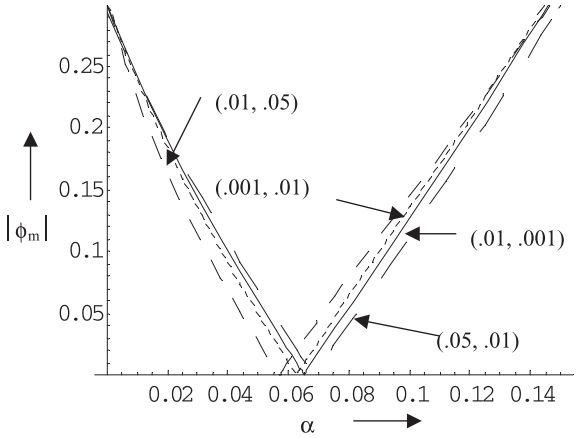

Fig. 18. Variation of amplitude $|\phi_m|$ of ion-acoustic double-layers with density ratio α for different values of (σ_1, σ_2) with the following set of parameters: $\eta = 0.476$, $\beta = 0.2$, $Z_1 = Z_2 = 1$.

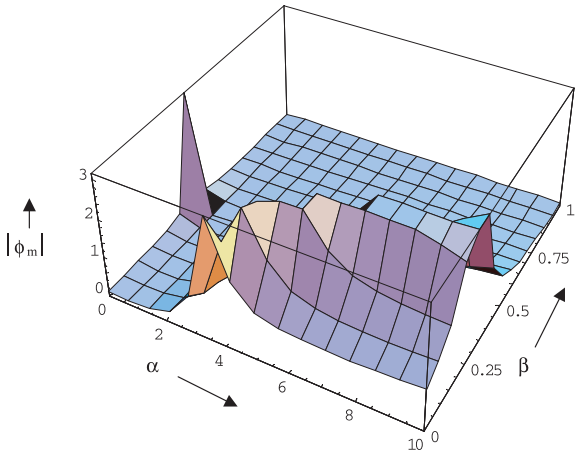

Fig. 19. 3D plot of fast ion-acoustic soliton for ϕ_m vs. α and β with $\eta = 1$, $\sigma_1 = 0.1$, $\sigma_2 = 0.01$, $Z_1 = Z_2 = 1$, and $u = 0.01$.

For studying double-layer solution, we plot $V(\phi)$ as a function of ϕ for $\alpha = 0.65$, $\beta = 0$ and for four different values of σ_1 and σ_2. Different double-layer solutions are obtained as shown in Figure 15 for (Ar^+, SF_6^-). However as we introduce the finite β, contributions of σ_1 and σ_2 do not play significant role in characterizing different double-layers as all the graphs converge to a single curve indicating only compressive double-layers for (Ar^+, SF_6^-) as depicted in Figure 16. It is clear from the expression of phase velocity of fast and slow modes, the increase in β leads to dominance of first term in the parenthesis of the phase velocity over the second term which is a function of σ_1 and σ_2. Density ratio plays a significant role in describing the dynamics of double-layers. To study this effect, we plot ϕ_m and width as a function of α with other values of parameters are $\sigma_1 = 0.01, \sigma_2 = 0.001$ and $\beta = 0.2$. The results are shown in Figures 17 and 18. In the case of (Ar^+, F^-) plasma, the results are very similar to case of $\beta = 0$ [28]. However, no double-layers are obtained as we further increase β.

To enrich the presentation, we have displayed 3D profile in Figure 19 where we have plotted ϕ_m as a function of α and β.

8 Conclusions

In this paper, we have studied the effect of non-thermal electrons on solitary waves and double-layers in a multispecies plasma consisting positive and negative ions with finite temperatures. The results are summarized as follows:

(i) for slow ion-acoustic mode, relative temperature of two ion species and finite β are relevant parameters. When $\sigma_1 > \sigma_2$, we obtain compressive as well as rarefactive solitons for different β. In case of (H^+, H^-) plasma, and in the absence of non-thermal electrons ($\beta = 0$), only compressive solitons are obtained. As β is increased to $\beta = 0.5$, we obtain a transition in which rarefactive solitons are obtained which disappear with further increase in β. For the fast

ion-acoustic mode, both compressive as well as rarefactive ion-acoustic solitons exist. With increase in nonthermalcity, there is transition with β and maximum occurs for low relative density concentration;

(ii) for (Ar^+, F^-) and (H^+, H^-) plasmas, where $\mu \leq 1$, we obtain rarefactive solitons. Finite β restricts the range of parameter space for obtaining solitons. Maximum peak amplitude and depth of the potential decrease with increase in the value of β. Maximum amplitude is obtained in the absence of nonthermal electrons;

(iii) for (H^+, O_2^-) plasma, behaviour is similar to that observed for (H^+, H^-). The role of mass ratio and finite β is very crucial in this case. For low value of β and increase mass ratio in (H^+, O_2^-) plasma system, only compressive solitons are obtained. However, when β is increased to 0.5, the rarefactive solitons are observed. However rarefactive solitons occur at higher β when mass ratio is increased;

(iv) for $\beta = 0$, different double-layers exist. Introducing finite β leads to appearance of a single double-layer solution;

(v) relative density (α) plays an important role when $\beta = 0$. However, as β is increased, no double-layer exists.

References

1. H. Alfven, P. Carlqvist, Sol. Phys. **1**, 220 (1967)
2. M. Temerin, K. Cerny, W. Lotko, F.S. Mozer, Phys. Rev. Lett. **48**, 1175 (1982)
3. L.E. Borovsky, J. Geophys. Res. **89**, 2251 (1984)
4. P. Carlqvist, IEEE Trans. Plasma Sci. **PS-14**, 794 (1986)
5. M.K. Mishra, A.K. Arora, R.S. Chhabra, Phys. Rev. E **66**, 46402 (2002)
6. K.S. Goswami, S. Bujarbarua, Phys. Lett. **108A**, 149 (1985)
7. R. Bharuthram, P.K. Shukla, Phys. Fluids **29**, 3214 (1986)
8. S.L. Jain, R.S. Tiwari, S.R. Sharma, Can. J. Phys. **68**, 474 (1990)
9. L.L. Yadav, S.R. Sharma, Phys. Scripta **43**, 106 (1991)
10. G.C. Das, S.G. Tagare, Plasma Phys. **17**, 1025 (1975)
11. S. Watanabe, J. Phys. Soc. Jpn **53**, 950 (1984)
12. S.G. Tagare, J. Plasma Phys. **36**, 301 (1986)
13. S.G. Tagare, R.V. Reddy, Plasma Phys. Control. Fusion **29**, 671 (1987)
14. F.B. Rizzato, R.S. Schneider, D. Dillenburg, Plasma Phys. Control. Fusion **29**, 1127 (1987)
15. F. Verheest, J. Plasma Phys. **39**, 71 (1988)
16. B.C. Kalita, M.K. Kalita, Phys. Fluids B **2**, 674 (1990)
17. B.C. Kalita, N. Devi, Phys. Fluids B **5**, 440 (1993)
18. M.K. Mishra, R.S. Chhabra, S.R. Sharma, J. Plasma Phys. **52**, 409 (1994)
19. K. Mishra, R.S. Chhabra, Phys. Plasmas **3**, 4446 (1996)
20. R.A. Cairns, A.A. Mamun, R. Bingham, R. Bostrum, R.O. Dendy, C.M.C. Nairn, P.K. Shukla, Geo. Phys. Res. Lett. **22**, 2709 (1995)
21. H. Schamel, Plasma Phys. **14**, 905 (1972)
22. H. Schamel, J. Plasma Phys. **9**, 377 (1973)
23. H. Schamel, Phys. Plasmas **7**, 4831 (2000)
24. A. Bandyopadhyay, K.P. Das, Phys. Scripta **61**, 92 (2000)
25. A. Bandyopadhyay, K.P. Das, Phys. Scripta **63**, 145 (2001)
26. A.A. Mamun, Eur. Phys. J. D **11**, 143 (2000)
27. T.S. Gill, H. Kaur, N.P.S. Saini, Phys. Plasmas **10**, 3927 (2003)
28. M.K. Mishra, A.K. Arora, R.S. Chhabra, Phys. Rev. E **66**, 046402 (2002)
29. Y.N. Nejoh, Phys. Plasmas **4**, 2813 (1997)
30. R.A. Cairns, A.A. Mamun, R. Bingham, P.K. Shukla, Phys. Scripta **T63**, 80 (1996)
31. A.Y. Wong, D.L. Mamas, D. Arnush, Phys. Fluids **18**, 1489 (1975)
32. H.J. Doucet, Phys. Lett. **33A**, 283 (1970)
33. Y. Nakamura, in *Nonlinear and Environmental Electromagnetics,* edited by H. Kikuchi (Elsevier, Newyork, 1985)
34. R.L. Merlino, J.J. Loomis, Phys. Fluids B **2**, 2865 (1990)